International Journal of Aeronautical and Space Sciences
https://doi.org/10.1007/s42405-022-00539-3

IJASS International Journal of Aeronautical and Space Sciences

ORIGINAL PAPER

Extracting Flight Plans from Recorded ADS-B Trajectories

Hyeonwoong Lee[1] · **Hak-Tae Lee**[1]

Received: 15 November 2021 / Revised: 6 April 2022 / Accepted: 22 September 2022

Abstract
Historic aircraft trajectory data are valuable resources for various research in the field of air traffic management. With the widespread use of Automatic Dependent Surveillance-Broadcast (ADS-B), these data are relatively easier to obtain. However, there are instances, where the original flight plans that do not contain controller interventions are necessary, such as developing scenarios for Human-in-The-Loop (HiTL) simulations. Even though the air traffic control system keeps records of the flight plan data, they are more difficult to obtain and often are not in the correct format to be applied to simulations. In this study, an algorithm is developed, which can extract the flight plan from recorded ADS-B trajectory and the Aeronautical Information Publication (AIP) that contains all the route and procedure information. The algorithm was validated against HiTL simulation results, where both the resulting trajectories with controller interventions and the original flight plans are available and showed a 98 percent success rate. The algorithms are applied to find the flight plans of about one million flights in the year 2019 that contain trajectory points inside the Incheon Flight Information Region (FIR). This flight plan extraction algorithm will be useful not only for the fast-time or real-time simulations of the air traffic but also for aviation safety-related research areas, where the controller-pilot interactions are important.

Keywords Original flight plan · ADS-B trajectories · AIP · HiTL simulation · Dijkstra algorithm

1 Introduction

To address the growing air traffic volume, the International Civil Aviation Organization (ICAO) established a future aviation system road map, Aviation System Block Upgrades (ASBU) through Global Air Navigation Plan (GANP) [1]. ASBU provides guidelines to achieve the harmonization of the Air Traffic Management (ATM) system between the member countries. Many different countries or regions around the world are developing their future ATM system according to their unique traffic environments. Some of the examples include the NextGen program of the USA [2] and the Single European Sky ATM Research (SESAR) of the European Union [3].

Mixed operations of manned and Remotely Piloted Aircraft System (RPAS) in the Korean National Airspace System is one of the major research topics in the Republic of Korea. Among many sub-topics of RPAS integration research, the need for flight plan extraction was raised while focusing on the HiTL simulations. Some of the early research used the recorded trajectories that contain radar vectoring for the simulation scenarios [4]. The recorded trajectories were simplified using a Ramer–Douglas–Peucker algorithm in both the horizontal dimension and vertical dimension to generate a list of waypoints for the simulation [5]. The prototype of the current flight plan extraction algorithm was first introduced in [6] and used for generating scenarios for subsequent work [7]. This prototype focused on finding the departure and arrival procedures within the terminal area.

The flight plan extraction algorithm described in this paper first generates multiple routes that consist of fixes, routes, and procedures specified in the AIP between the beginning and ending trajectory points. These candidate routes are scored based on the number of the recorded trajectory points within the candidate route boundaries while dynamically varying the size of the boundaries. The route with the highest score is selected as the flight plan.

The algorithm was validated against a set of recorded trajectory data from HiTL simulations [8] of lost communication situations of RPAs in busy terminal airspace that includes

✉ Hak-Tae Lee
haktae.lee@inha.ac.kr

Hyeonwoong Lee
hyeonwoong.lee@inha.edu

[1] Aerospace Engineering, Inha University, 36 Gaetbul-Ro, Yeonsoo-Gu, Incheon 21999, Republic of Korea

Published online: 29 October 2022

the Incheon International Airport (RKSI) and the Gimpo International Airport (RKSS) of the Republic of Korea. The algorithm demonstrated about 98 percent success rate.

For further validation and application of the algorithm, the entire set of trajectories, around one million flights, that were captured inside the Incheon Flight Information Region (FIR) was processed. Even though it is not possible to verify every case, the algorithm was robust enough to generate a fairly convincing flight plan for every single trajectory. The results will be used to analyze the impacts of RPAS integration as well as radar vectoring patterns and related risks as an extension to the work by the authors [8–10].

Following this Introduction, Sect. 2 explains the characteristics of the ADS-B trajectory data. Section 3 describes the AIP data, information about fixes, arrival and departure procedures, and routes in detail. The algorithm is presented in Sect. 4. Section 5 presents the results of the validation. In Sect. 6, selected cases from the large-scale application of this algorithm are presented and discussed. Finally, Sect. 7 concludes this paper.

2 ADS-B Trajectory

The recorded trajectories used in this paper are rearranged ADS-B data purchased from FlightAware [11]. The data set includes all the flights in the year 2019 that has at least a single trajectory point within the Incheon FIR boundary. For each flight, the full trajectory from departure to arrival is available including the names of the origin and destination airports. Table 1 shows a sample of the trajectory data for a single flight. Latitude, longitude, and ground track angle denoted by LAT, LON, and TRK, are used for the flight plan extraction algorithm along with the origin and destination airport information.

Airport information is used to infer the corresponding AIP data for the given airport. For the current study, only the AIP data of Korean National Airspace is used.

In the previous research [6], three-dimensional trajectory including the altitude was used. However, it was discovered that using only the two-dimensional information is sufficiently accurate while significantly reducing the computational cost.

3 Route Information

In this section, navigation elements used for the flight plan extraction algorithm are defined. The information is publicly available through AIP [12] by the Ministry of Land, Infrastructure and Transport.

3.1 Fixes

In AIP, two types of points exist, fix and waypoint. the fix has latitude and longitude coordinates, while the waypoint contains additional information, such as altitude or designated speed. Because the current algorithm uses only two-dimensional coordinates, both the fix and waypoint are referred to as a fix in the rest of this paper. A fix contains its name, latitude, and longitude.

3.2 Route Segments

Route segment is a newly defined element, which is a straight line segment between two fixes, as shown in Fig. 1. It consists of an entry fix (FIX 1), exit fix (FIX 2), length (L), lateral limit (LL), course (CRS), and whether it is unidirectional or bidirectional (arrow symbols). LL is set through the flight condition of the Area Navigation (RNAV) of each route. For example, if a route segment j is set to RNAV5, the LL of this segment, LL_j, is 5 NM. For route segments that are part of arrival or departure procedures, the LL is set to 1 NM. If the route segment is a part of an Instrument Landing System (ILS) approach procedure, it is set to 0.33 NM.

3.3 Instrument Flight Procedures (IFP)

IFP refers to a procedure established to ensure the safety of an aircraft from obstacles, while the aircraft is flying under the Instrument Flight Rule (IFR). It is established in consideration of the airport and the surrounding environments. In the

Table 1 Sample trajectory data

Callsign:	AAR136					
Origin:	RKSI					
Destination:	RJFF					
Time (HH:mm:ss)	LAT (deg)	LON (deg)	ALT (ft)	GSD (knot)	VRT (ft/min)	TRK (deg)
18:31:16	37.4822	126.436	775	159	0	325
18:31:51	37.5031	126.418	2425	155	2294	326
18:32:09	37.5144	126.409	3050	166	1853	327
18:32:25	37.52426	126.4006	3475	181	1583	327

LAT, Latitude; LON, Longitude; ALT, Altitude; GSD, Ground Speed; VRT, Vertical Rate; TRK, Track Angle

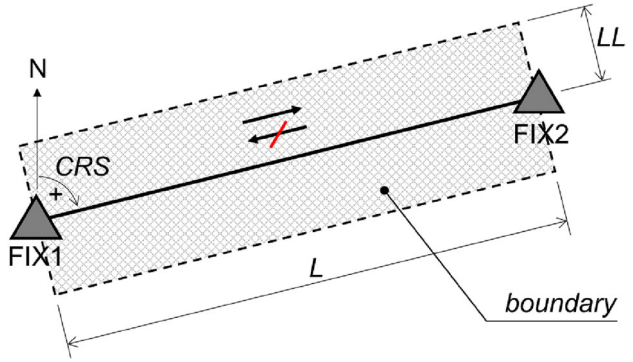

Fig. 1 Route segment definition

case of the Republic of Korea, when setting up IFPs, the flight procedures of ICAO's Doc-8168 (PANS-OPS: Aircraft Operations) are preferentially applied. In exceptional cases such as ground obstacles or military zones, the Terminal Instrument Procedures of the Federal Aviation Administration [13–15] are adapted.

For a given airport, IFP can be divided into departure or arrival procedures and expressed as a sequence of route segments. In this paper, departure procedure refers to a connection between a departure runway and a Standard Instrument Departure (SID). If multiple runways are connected to a single SID, each combination is considered a separate departure procedure. Similar to the departure procedures, arrival procedure refers to a connection between a Standard Instrument Arrival (STAR) and an ILS approach procedure for a specific runway. Figure 2 shows an example, where a STAR is connected to two different approach procedures, one for each runway. These are considered two different arrival procedures.

IFPs are updated depending on the airspace environments or airport conditions. Therefore, start and end dates must be compared with the date of the trajectory when executing the algorithm. Table 2 shows the data structure of an arrival procedure generated from AIP for the flight plan extraction algorithm. In this paper, full data set for arrival and departure procedures are constructed for the three busiest airports: RKSI, RKSS, and Jeju International Airport (RKPC).

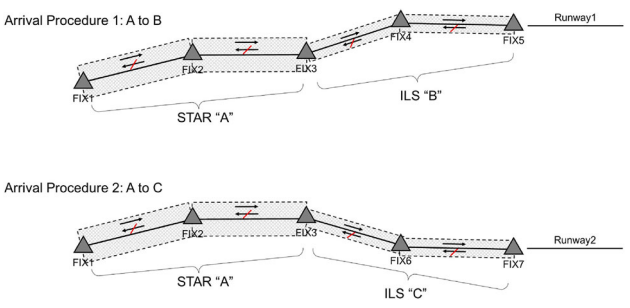

Fig. 2 Arrival procedure construction

Table 2 Example data structure of an arrival procedure

Parameter		Value
Name		RNAV GUKDO 1N to ILS/LOC approach to RWY 15R
Type		Arrival procedure
Airport		RKSI (Incheon Intl' Airport)
Route segments		16 route segments
Effective date	Start	16 FEB 2017
	End	8 APR 2021

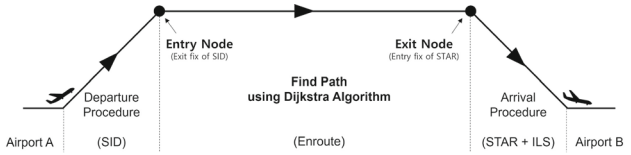

Fig. 3 Three portions of the flight plan

3.4 Enroute

Portions of the routes between the last fix of SID to the first fix of STAR are referred to as enroute. In the Republic of Korea, enroute consists of lower ATS routes and RNAV routes. Some of the route segments in the enroute portion has multiple RNAV performance conditions depending on the jet route it belongs to. In this case, the largest one is chosen for the LL of the particular segment for the flight plan extraction algorithm.

Figure 3 shows the complete picture of a candidate flight plan. The departure procedure is from the departure runway to the exit node of SID, which is the entry node to enroute. Enroute is from the entry node to the exit node, which is the first fix of the STAR. The Arrival procedure is from the first fix of STAR via the connected ILS approach procedure to the landing runway. Figure 4 shows the entire enroute portion within the Incheon FIR.

4 Flight Plan Extraction Algorithm

In this section, a detailed process for scoring and selecting the flight plan is described.

For a given trajectory, the flight plan extraction algorithm first finds the candidate departure and arrival procedures and then connects the two by finding the shortest paths. Among multiple candidate routes from the departure runway to the arrival runway, the one with the highest score is selected as the flight plan.

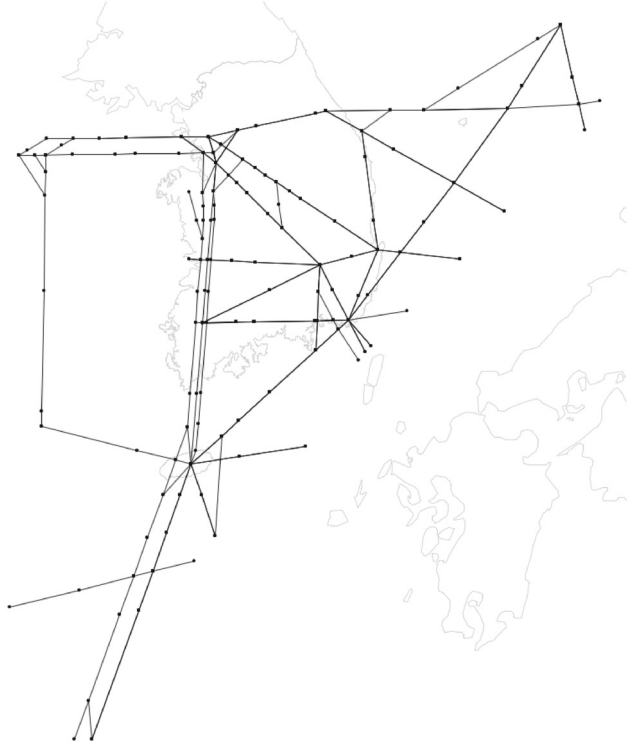

Fig. 4 Enroute fixes and route segments graph

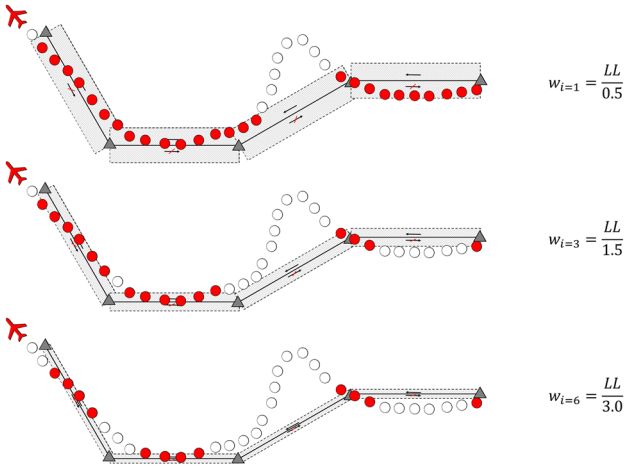

Fig. 5 Route scoring process

4.1 Route Scoring

Route scoring is a method used throughout this paper to quantify the similarity between a recorded trajectory and a sequence of route segments. As shown in Fig. 5, the number of points within the route segment boundaries are counted, while progressively reducing the width, w, by scaling the original LL of the corresponding route segment. Various weighting factors are applied based on width of the boundary and the matching between the directions of flight and route segments.

Equation (1) describes how the initial score is calculated for a given set of route segments, $\{r_j\}$, where $1 \leq j \leq N_r$, and a trajectory, $\{p_k\}$, where $1 \leq k \leq N_t$. N_r is the total number of route segments in a given candidate route, and N_t is the total number of track points in a given flight. Each route segment r_j contains information shown in Fig. 1, while a track point, p_k, contains latitude, longitude, and track angle as shown in Table 1.

$$S_0 = \sum_{i}^{10} \sum_{j}^{N_r} \sum_{k}^{N_t} \frac{\mathrm{INT}\left(w_{ij}, r_j, p_k\right)}{{w_{ij}}^2} F\left(r_j, p_k\right). \tag{1}$$

The first summation over the index i represents the decreasing the size of the boundary by dividing the LL by a scaling factor, f_i, as shown in Eq. (2). f_i increases from 0.5 to 5.0 with a step size of 0.5. The reason why f_i starts at 0.5 is to capture points that are outside the allowed RNAV limits, which are very likely to be caused by the controller's vectoring instructions. Any track point inside the route segment boundary with a smaller w_{ij} has a larger contribution to the total score.

$$w_{ij} = \frac{LL_j}{f_i}. \tag{2}$$

The function INT denotes whether a point p_k is an interior point of the route segment r_j when the lateral boundary is given by w_{ij}, as shown in Eq. (3):

$$\mathrm{INT}\left(w_{ij}, r_j, p_k\right) = \begin{cases} 1, (p_k \text{ is inside the boundary of} \\ \quad r_j \text{ set by } w_{ij}) \\ 0, (\text{otherwise}). \end{cases} \tag{3}$$

Weighting factor for the difference in the course, F, is computed using Eq. (4), where the course error, e_c, is defined the absolute value of the difference between the track angle, t_k, of the point p_k and the course, c_j, of the route segment r_j. Maximum course error, $e_{\max}$, is set at 45 degrees. If the maximum course error is too small, correct candidate flight plan routes tend to get lower scores. On the other hand, if this value is too large, number of cases, where an irrelevant flight plan route in the vicinity getting higher score increases. 45 degrees show a good balance between the two.

$$F\left(r_j, p_k\right) = \begin{cases} 1 - \frac{e_c}{e_{\max}}, & (e_c < e_{\max}) \\ 0, & (e_c \geq e_{\max}), \end{cases} \tag{4}$$

$$e_c = \left\| c_j - t_k \right\|. \tag{5}$$

Finally, this initial score, S_0, is scaled, as shown in Eq. (6). N_c denotes the number of route segments that contain at least

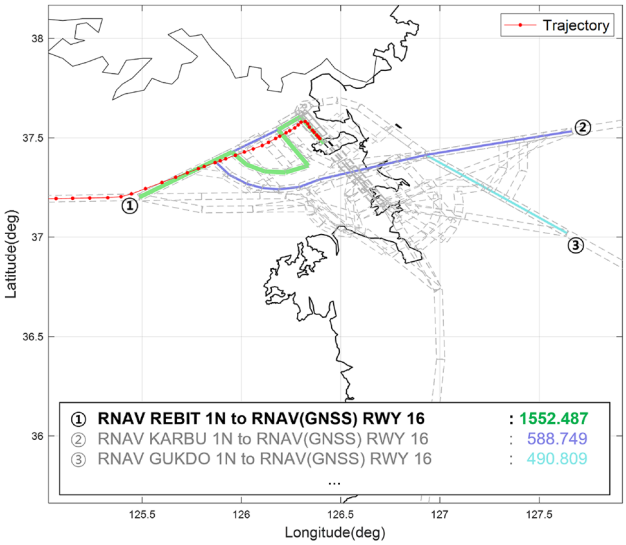

Fig. 6 Route scoring example

one trajectory point regardless of the w_{ij}. Without this scaling, candidate routes with a larger number of route segments get higher scores regardless of how well the shapes match.

$$S = S_0 \left(\frac{N_c}{N_r} \right)^2. \tag{6}$$

Figure 6 shows calculated scores for 3 arrival procedures to RKSI using the sample trajectory marked in red. As can be observed, the RNAV REBIT 1N procedure that matches the trajectory better than the others results in a much higher score.

4.2 Scoring of the Full Candidate Route

All departure procedures described in Sect. 3.3 that correspond to the origin airport of the flight are scored according to the scoring algorithm. These scores are normalized again by the maximum score so that the scores for the departure procedures are in between zero and one. All arrival procedures corresponding to the destination airport of the flight, which are combinations of STARs and ILS approach procedures, are also scored and normalized similar to the departure procedures.

$$\bar{S}_i = \frac{S_i}{\max\{S_i\}}. \tag{7}$$

Between a departure procedure, P_{di}, and an arrival procedure, P_{aj}, the enroute portion of the route is generated by finding the minimum distance path between the end of the SID of P_{di} and the beginning of the STAR of P_{aj}. In this paper, the Dijkstra algorithm is used to find the minimum distance path. This enroute portion is separately scored, but it is not normalized.

With m departure procedures and n arrival procedures, a total of mn candidate routes are created for a flight between the origin and the destination airport. For each complete candidate route, the final score is calculated by multiplying the three scores, as shown in Eq. (8). Among the mn candidates, the one with the highest score is selected as the original flight plan.

$$S_{\text{full}} = \bar{S}_{\text{dep}} \times S_{\text{enr}} \times \bar{S}_{\text{arr}}. \tag{8}$$

As mentioned in Sect. 3.3, full departure and arrival procedures are constructed from AIP for only three airports. For all the other airports, the first or last point inside the Incheon FIR from the trajectory becomes the starting or ending point. All the fixes within 20 NM of these starting or ending points are identified and become one end or both ends of the candidate routes. The scoring process is identical for these cases.

5 Validation

To test the flight plan extraction algorithm, the results of HiTL simulations [8] conducted by the authors in August 2021 were used. These simulations were designed to assess the impacts of RPAs with a lost C2 link in busy terminal airspace, which naturally caused severe radar vectoring. Because the simulations must start from detailed flight plans, it was possible to compare the extracted flight plans from the vectored trajectory with the original flight plans.

The HiTL simulations consist of two scenarios with around 150 flights that take about 1 h each. Three active controllers and nine pseudo pilots participated. A total of six simulation sessions were completed, and a total of 246 flights longer than 10 min were identified as the cases for comparison. Among the 252 flights, the proposed algorithm extracted the correct flight plan for 246 flights, which translates to a 97.8% success rate.

Figure 7 shows a typical case, where the correct original flight plan is found by the algorithm. The red line is the trajectory that includes all the vectoring by the air traffic controller. The green line is the extracted flight plan, which is identical to the original flight plan route. Figure 8 shows a case, where the algorithm failed. The flight has entered the STAR but the simulation ended before it landed, and there was not enough information to recover the STAR. All six failure cases were caused by the lack of trajectory data not by the intrinsic limitation of the proposed algorithm.

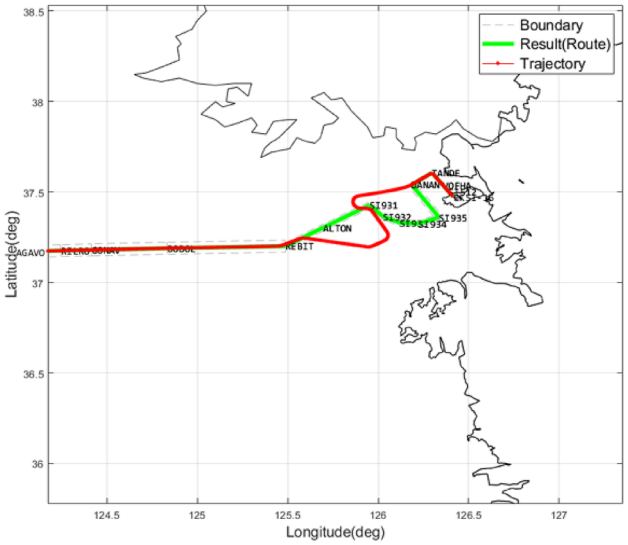

Fig. 7 Example success case

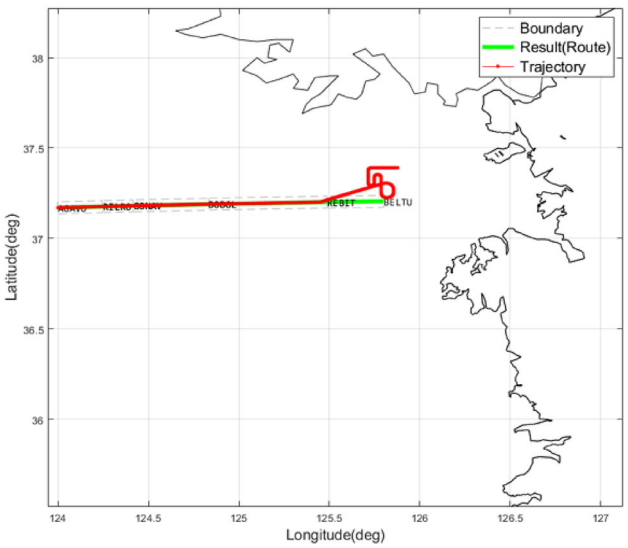

Fig. 8 Example failure case

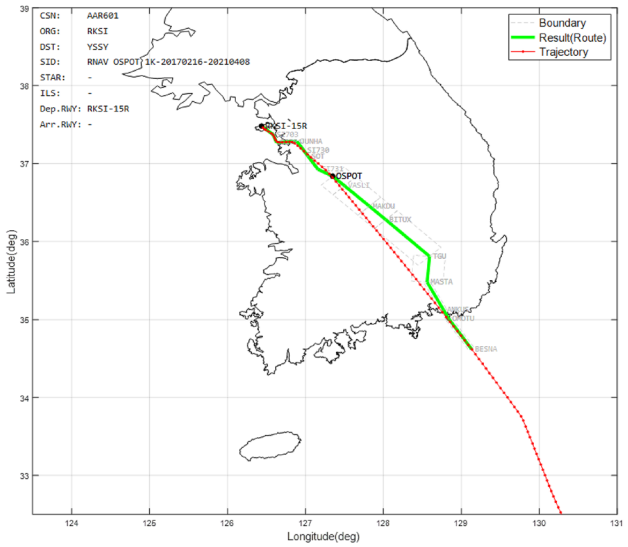

Fig. 9 RKSI departure example

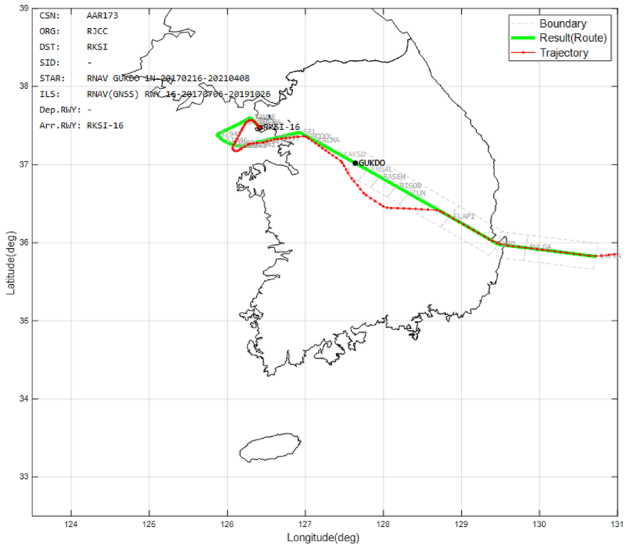

Fig. 10 RKSI arrival example

6 Results and Discussion

The proposed algorithm successfully processed the ADS-B trajectory data of one million flights in the year 2019, which shows that the algorithm is robust. Although it is not possible to verify each individual case, the below subsections present some of the representative cases.

6.1 Departures and Arrivals to and from RKSI

As almost all of the flights originating from or terminating at RKSI are international flights, extracted flight plans are between the Incheon FIR boundary and the airport.

Figure 9 shows an example case, where a flight departs RKSI from runway 15R and flies to Sydney Airport in Australia. The extracted flight plan from RKSI to BESNA fix, the point of entry into Fukuoka FIR of Japan, is expressed in green. As there is no straight route specified in AIP from OSPOT fix to BESNA fix, it is highly probable that the flight received a direct-to BESNA instruction from the Air Traffic Controller (ATC) at OSPOT, the last fix of the SID, RNAV OSPOT 1K.

Figure 10 shows the trajectory and extracted flight plan of a flight departing from Shinchitose Airport in Japan and arriving at RKSI. Based on the extracted flight plan, this trajectory shows a path-stretch in the enroute portion between the ELAPI fix and the KAKSO fix. It can also be observed

that the flight was directed to DANAN fix while on the point merge arc of the RNAV GUKDO 1N arrival procedure.

As in the two example cases, if airport flight procedures are incorporated, sufficiently valid flight plans down to the runway level can be extracted even with heavily vectored flights.

6.2 Domestic Flights

Figures 11 and 12 show two examples between RKSS and RKPC, where full airport procedure data were available. As mentioned, if both departure and arrival airport flight procedure information exist, the original flight plan for all sections, including departure runway, SID, Enroute, STAR, ILS, and arrival runway can be extracted.

Figure 11 shows the extracted flight plan of flight AAR8911 departing from runway 14L of RKSS and arriving at runway 07 of RKPC. In this result, BULTI fix to DOTOL fix section corresponding to the enroute portion is a part of the Y711 route, which is known as the second busiest route in the world as of 2010 [16]. The actual trajectory in Fig. 11 shows a significant detour towards the Yellow Sea, which is likely to be caused by the congestion on Y711. It can be observed that even with a significant amount of detour, the algorithm found the highly probable original flight plan.

Figure 12 shows the result of flight plan extraction for flight AAR8911 departing from runway 07 of RKPC and arriving at runway 14R of RKSS. This trajectory shows a typical vectoring pattern of a flight that transitions from the Y722 route to the RNAV OLMEN 1D STAR of RKSS, which is taking a shortcut to the KALMA fix.

6.3 No Flight Procedure Information at Departure and Arrival Airports

Figures 13 and 14 show the extraction examples when the flight procedure information is not available at both the departure and arrival airports. As previously mentioned, they will only have the enroute portion of the flight plan.

Figure 13 shows the extracted flight plan for the AAL180 flight departing from Beijing Capital International Airport (ZBAA) in China and arriving at Los Angeles International Airport in the United States. In the case of this trajectory, it is simply an aircraft passing through Incheon FIR, and the results are shown for the flight section from the AGAVO fix, an entry point to Incheon FIR from Shanghai FIR in China, to the LANAT fix, an exit fix from Incheon FIR to Fukuoka FIR in Japan. The extraction results show that the aircraft flew along the Y644 route and transitioned to the Y697 route from the EGOBA fix.

Figure 14 shows the flight plan extraction result of flight AAR315, which departs from Gimhae International Airport (RKPK) and arrives at ZBAA. In this paper, the flight procedure information of RKPK was not applied, so the route was extracted for the enroute portion from near RKPK to the Incheon FIR boundary.

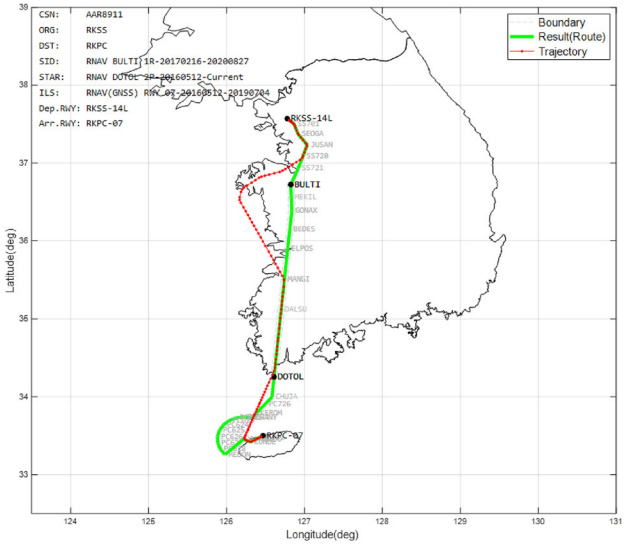

Fig. 11 RKSS to RKPC example

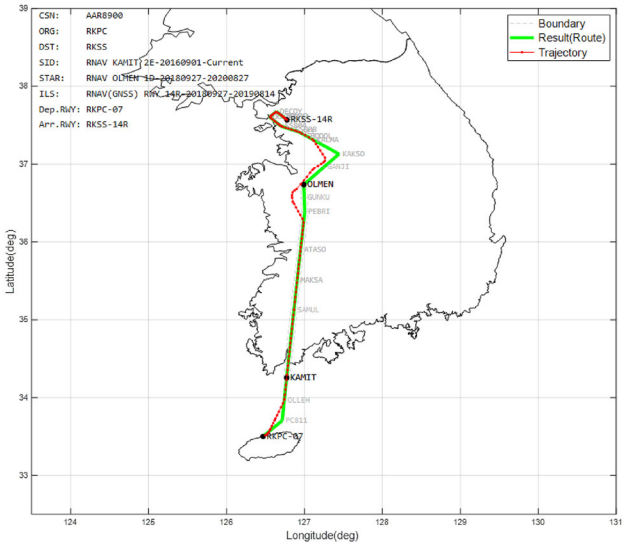

Fig. 12 RKPC to RKSS example

6.4 Limitations

Although the extracted flight plans are highly convincing, several patterns have been identified that display the limitations of the proposed algorithm. The first pattern where the proposed algorithm struggles to correctly identify the original flight plan happens when a specific procedure is assigned for a particular flow direction. Figure 15 shows an example, where the RNAV OLMEN 1N procedure that should be used by the flights coming from the South was extracted for a

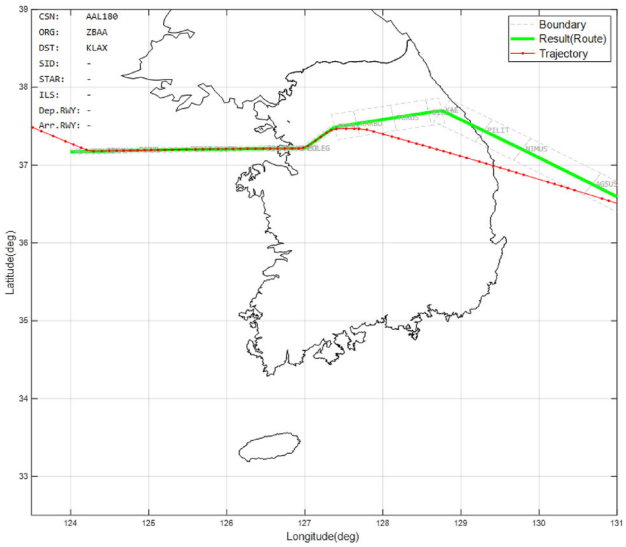

Fig. 13 Transiting flight example

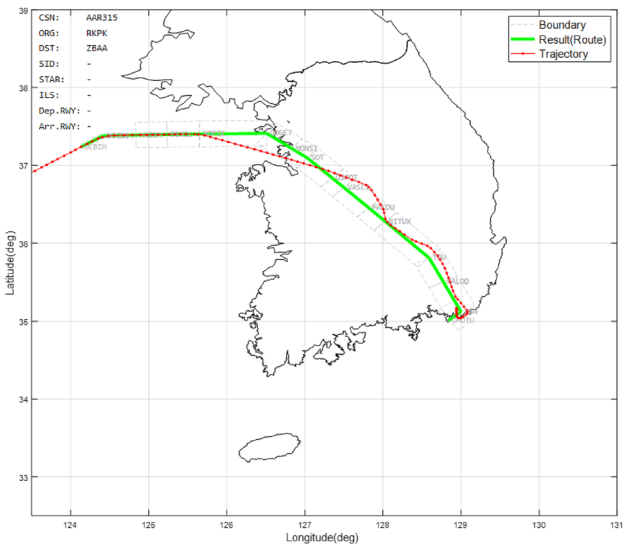

Fig. 14 International arrival at RKPK

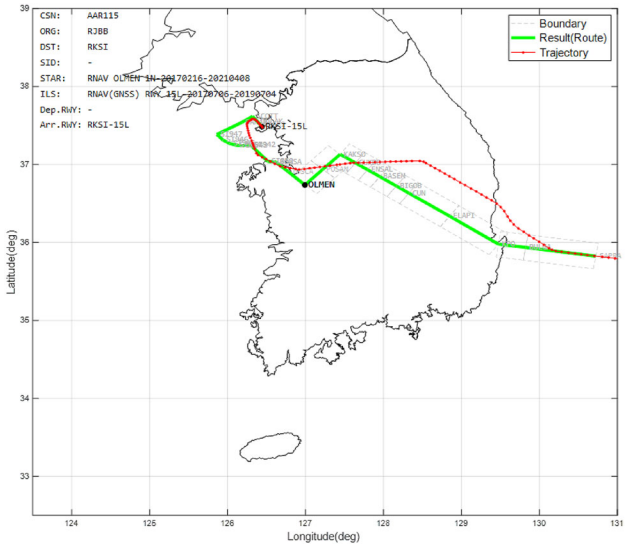

Fig. 15 Assigned flow direction

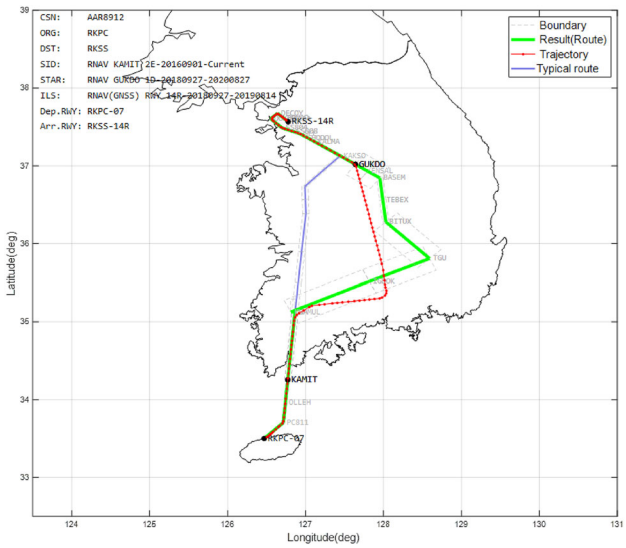

Fig. 16 Unusual detour

flight that is coming from the East. This was due to the flight being vectored by ATC flew a trajectory similar to the RNAV OLMEN 1N procedure. The second pattern happens when a path stretch or detour is so severe that another route exists in the vicinity of the path. An example shown in Fig. 16 is a flight from RKPC to RKSS, In addition to the enroute portion that is severely detoured, RNAV GUKDO 1D was extracted as the arrival procedure. On the contrary, flights from RKPC to RKSS usually uses the Y722 route and KAKSO as the entry fix to the STAR as shown in a purple line in Fig. 16. Even though the extracted routes are similar in shape to the flown trajectory, this is not likely to be the original flight plan for the flight.

7 Conclusions

This paper introduces a flight plan extraction algorithm developed to find the original flight plan from an actual trajectory that contains ATC interventions. The algorithm was validated through data acquired from HiTL simulations with a high success rate. The algorithm was applied to process around one million flights that were at least partially inside the Incheon FIR boundary in the year 2019. Even though it is not possible to confirm every single case, this algorithm will be very useful, especially, for statistical studies with a large amount of data. In addition, the proposed algorithm can be used for fast-time and real-time simulation-based studies in generating realistic scenarios based on historic data.

Acknowledgements This work is supported by the Korea Agency for Infrastructure Technology Advancement (KAIA) grand funded by the Ministry of Land, Infrastructure and Transport (Grant 21ATRP-C108186-07 and 22BDAS-B158275-03).

References

1. Doc I (2013) 9750-AN/963 Global Air Navigation Plan 2013–2028. ICAO, Montreal
2. Planning J et al (2007) Concept of operations for the next generation air transportation system. Technical Report
3. Consortium S et al (2012) European ATM master plan. Mar-2009
4. Kang J et al (2019) Safety and workload assessment of lost C2 link on Seoul–Jeju route. J Aerosp Inf Syst 16(4):120–131
5. Lee H, Park B-S, Lee H-T (2016) Waypoint extraction from recorded ADS-B trajectory data. In: 2016 The Korean Navigation Institute conference
6. Lee H, Park B-S, Lee H-T (2019) Analysis of alerting criteria and DAA sensor requirements in terminal area. In: 2019 IEEE/AIAA 38th digital avionics systems conference (DASC)
7. Lee H, Park S-H, Lee H-T (2020) Lost C2 link contingency procedures for Seoul TMA and assessment on safety and controller workload. In: 2020 IEEE/AIAA 39th digital avionics systems conference (DASC)
8. Lee H-T (2022) Assessment of safety, workload, and delay through HITL simulations for lost C2 link contingency procedure in ICN. In: ICAO WP, RPASP/19-WP/5
9. Lee H, Lee H-T (2020) Risk analysis of flight procedures at Incheon International Airport and Gimpo International Airport. J Adv Navig Technol 24(6):500–507
10. Lee H-T, Lee H (2020) Risk analysis of aircraft operations in Seoul TMA based on DAA well clear metrics using recorded ADS-B data. J Adv Navig Technol 24(6):527–532
11. FlightAware (2021) FlightAware-ADSB. https://flightaware.com/. Accessed 21 Oct 2021
12. Aeronautical Information Services (2021) Aeronautical information publication (E-AIP). http://aim.koca.go.kr/eaipPub/Package/history-en-GB.html. Accessed 21 Oct 2021
13. Doc I (2006) 8168 OPS/611 aircraft operations: procedures for air navigation services-volume II construction of visual and instrument flight procedures. ICAO, Montreal
14. FAA, M (2002) United states standard for terminal instrument procedures (TERPS), change 19
15. Jang I (2000) Instrument flight procedure of Incheon International Airport. J Aviat Dev Korea 24:62–82
16. Airportal (2021) Aviation statistics. https://www.airportal.go.kr/knowledge/statsnew/main.jsp. Accessed 21 Oct 2021